2D Free-standing Film-Inspired Electrocatalyst for Highly Efficient Hydrogen Production

Jian Gao, Zhihua Cheng, Changxiang Shao, Yang Zhao*, Zhipan Zhang and Liangti Qu*

Key Laboratory of Photoelectronic/Eletrophotonic Conversion Materials, School of Chemistry, Beijing Institute of Technology, Beijing 100081, P. R. China

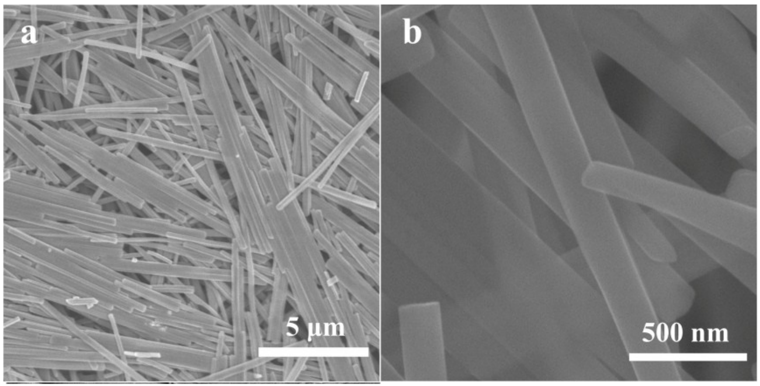

Figure S1 (a, b) The SEM images of the as-prepared molybdenum trioxide (MoO_3) nanoribbons.

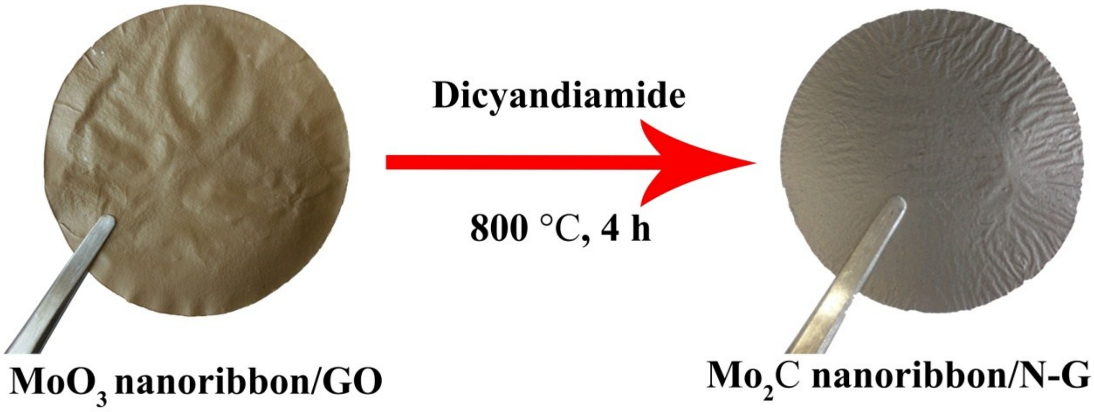

Figure S2 The photograph of the self-standing film prepared via a conversion from the MoO_3 nanoribbon/GO film (claybank color) and Mo_2C nanoribbon/N-G film (shiny metallic luster).

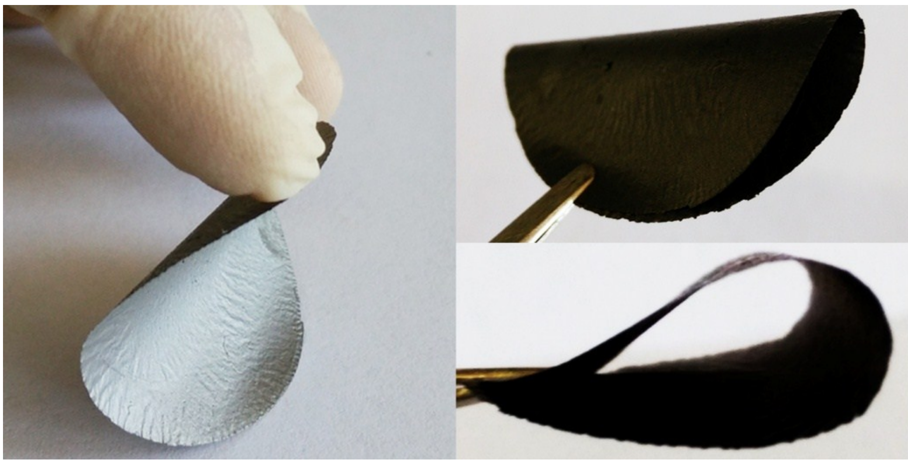

Figure S3 photographs of the free-standing Mo_2C nanoribbon/N-G film.

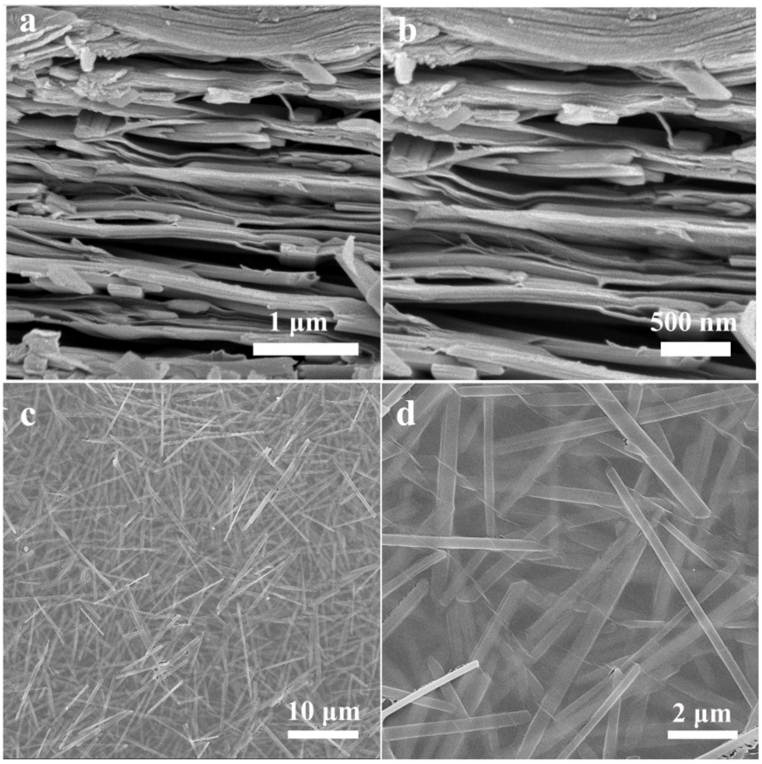

Figure S4 The SEM images of the cross-section (a, b) and top surface (c, d) of MoO_3 nanoribbon/GO film.

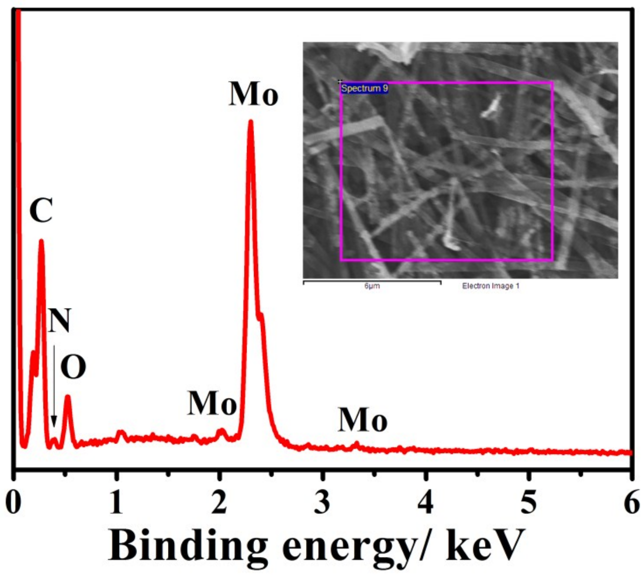

Figure S5 EDS spectrum of the Mo_2C nanoribbon/N-G film.

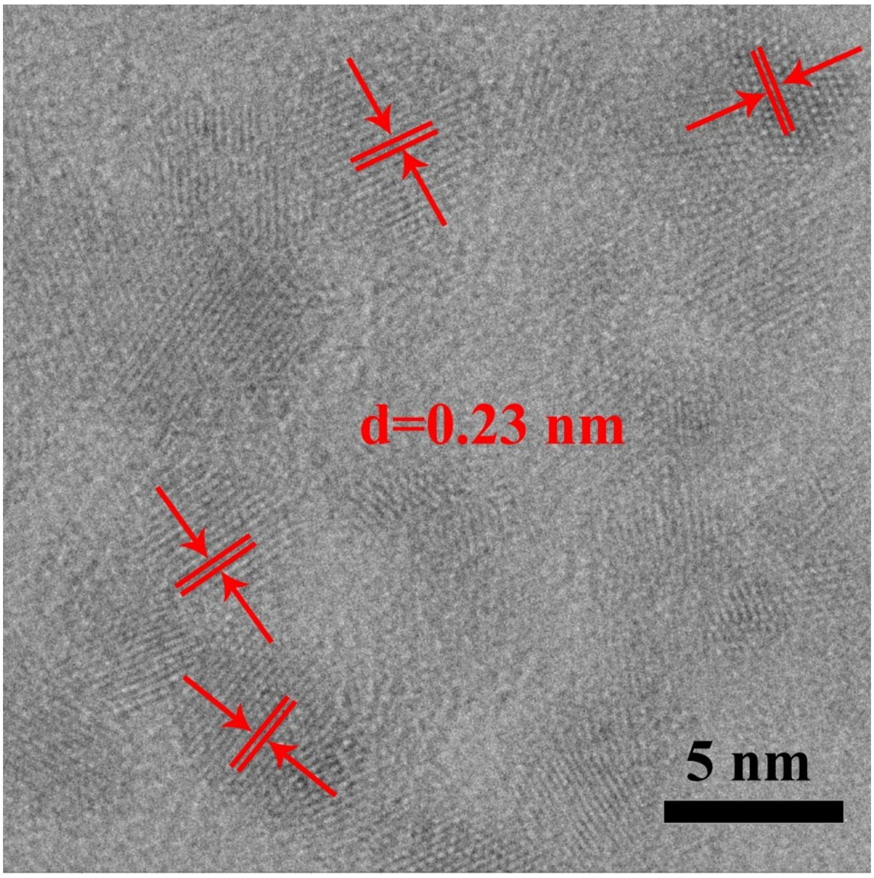

Figure S6 HR-TEM image of the Mo_2C nanocrystals on the surface of Mo_2C nanoribbon/N-G film.

Table S1 Elemental contents of Mo_2C nanoribbon/N-G film.

Samples	Mo/XPS (wt%)	C/XPS (wt%)	N/XPS (wt%)	O/XPS (wt%)
Mo_2C nanoribbon/N-G film	1.07	84.95	8.54	5.44

Table S2. Summary of representative non-noble metal based free-standing HER catalysts in acidic electrolyte.

Non-noble metal based free-standing catalysts	Onset overpotential mV	Current density mA cm^{-2}	Overpotential mV	Ref.
$NiSe_2$ nanowall/carbon cloth	120	10	145	1
Mo_2C nanobeads on Graphene-coated carbon nanofibers (G-CNF) membrane	115	10	188	2
3D graphene/ MoS_2 composites	110	50	200	3
Cu nanoparticles/carbon nanofibers hybrid	61	10	200	4
Monolayer MoS_2 films/3D nanoporous metals	118	10	226	5
NiO@C nanobelt	-	10	294	6
3D ReS_2/carbon foam	-	10	336	7
Mo_2C nanoribbon/N-G film	**84**	**10**	**162**	**This work**

Table S3. Summary of representative Mo_2C-based HER catalysts in acidic electrolyte.

Mo_2C-based HER catalyst	Current density	Overpotential	Reference
MoCN	10 mA cm^{-2}	145 mV	8
Mo_2C nanocrystal embedded N-doped carbon nanotubes	10 mA cm^{-2}	147 mV	9
Mo_2C nano-rod Ni impregnated Mo_2C nano-rod	10 mA cm^{-2}	150 mV	10
Mo_2C/CNT	10 mA cm^{-2}	~150 mV	11
Commercial Mo_2C	10 mA cm^{-2}	192 mV	12
Mo_2C nanoparticles	10 mA cm^{-2}	198 mV	13
Mo_2C nanowires	10 mA cm^{-2}	200 mV	14
Mo_2C Nanoparticles Decorated Graphitic Carbon Sheets	10 mA cm^{-2}	210 mV	15
Mo_2C-carbon nanocomposite	5 mA cm^{-2}	260 mV	16
Mo_2C nanoribbon/N-G film	**10 mA cm^{-2}**	**162 mV**	**This work**

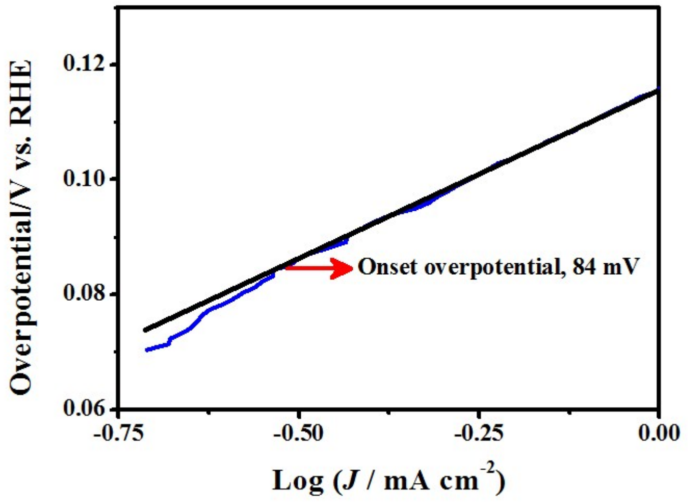

Figure S7 The Tafel plot of the Mo_2C nanoribbon/N-G film.

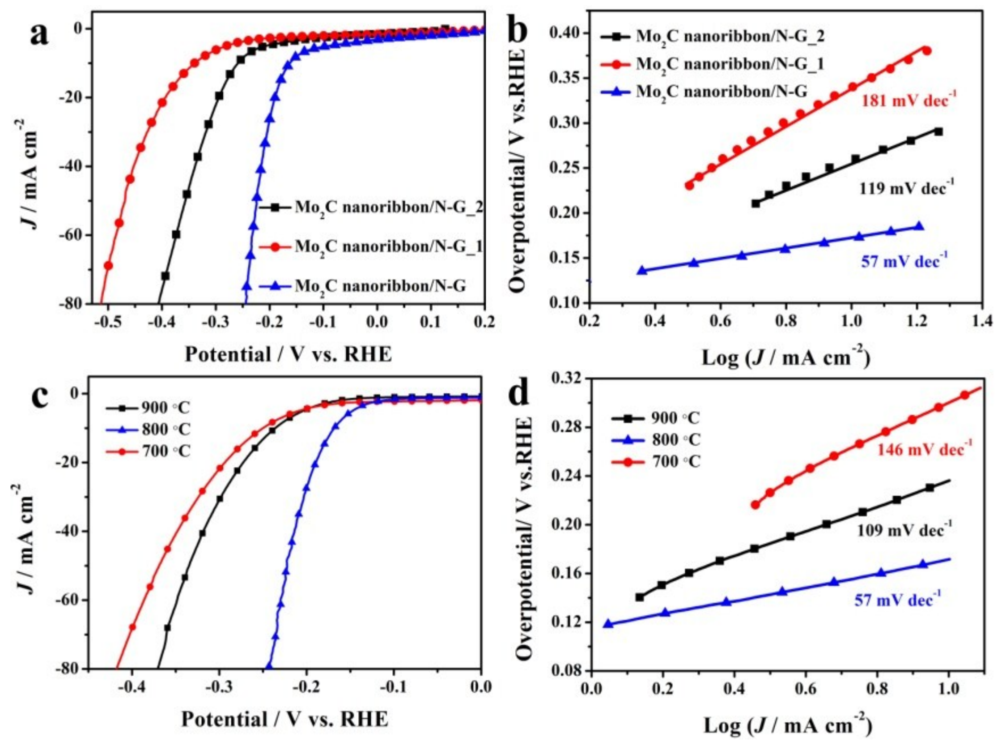

Figure S8 (a) Polarization curves and (b) Tafel plots of Mo_2C nanoribbon/N-G, Mo_2C nanoribbon/N-G_1 and Mo_2C nanoribbon/N-G_2 in 0.5 M H_2SO_4, respectively. (c) Polarization curves and (d) Tafel plots of Mo_2C nanoribbon/N-G at different carbonization temperature, respectively.

The weight percentage of MoO_3 nanoribbon in the Mo_2C nanoribbon/N-G film and calcination temperature play important role in HER properties. As shown in Figure S8a and b, the Mo_2C nanoribbon/N-G films with lower or higher weight percentage of MoO_3 nanoribbon are investigated. The corresponding samples are labeled as Mo_2C nanoribbon/N-G_1 (the weight ratio of MoO_3 nanoribbon to GO is 2:1) and Mo_2C nanoribbon/N-G_2 (the weight ratio of MoO_3 nanoribbon to GO is 8:1), respectively. However, both of the Mo_2C nanoribbon/N-G_1 and Mo_2C nanoribbon/N-G_2 exhibits poorer HER performance than that of the as-prepared Mo_2C nanoribbon/N-G (the weight percentage of MoO_3 nanoribbon is 5), which is probably due to the low electrocatalytic activity for the Mo_2C nanoribbon/N-G_1 and aggregation of Mo_2C nanoribbons in Mo_2C nanoribbon/N-G_2.

In addition, the Mo_2C nanoribbon/N-G film with different calcination temperatures (700 °C, 800 °C and 900 °C) are also studied. As demonstrated in Figure S8c and d, the Mo_2C nanoribbon/N-G film shows the increasing HER performance with the increase calcination temperature from 700 °C to 800 °C, probably attributed to efficient crystalline transformation of β-Mo_2C. However, when the calcination temperature reaches 900 °C, the as-prepared Mo_2C nanoribbon/N-G film exhibits a slight decrease of the HER performance, probably due to the loss of N element at high treating temperature.

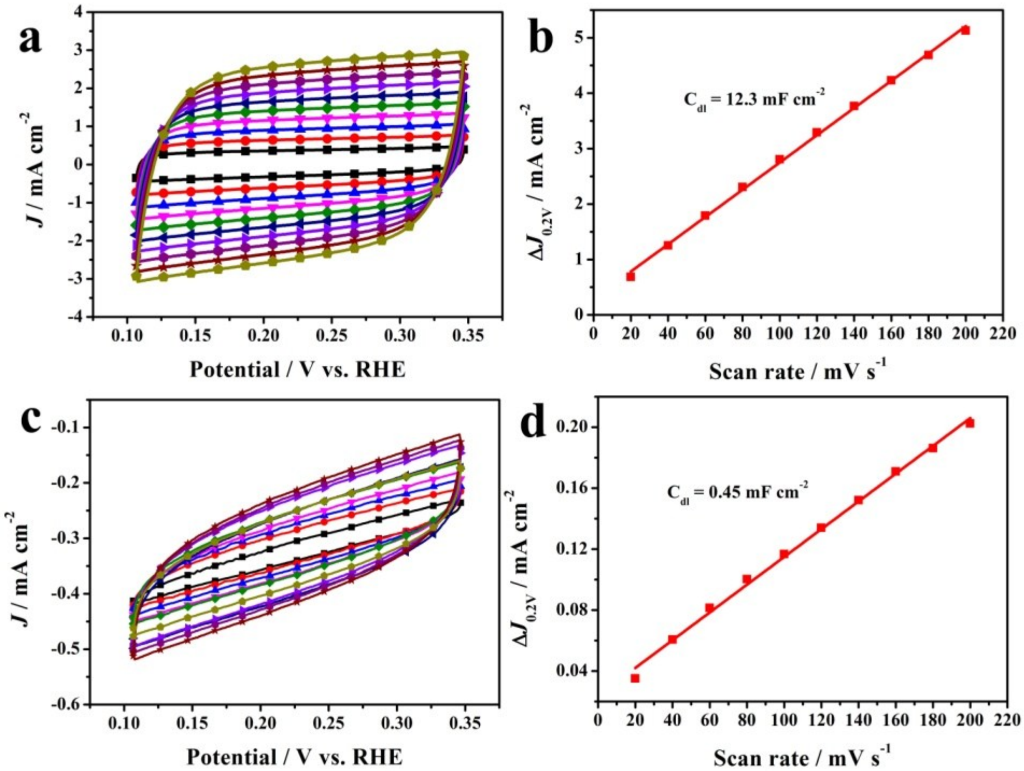

Figure S9 The cyclic voltammetry (CV) of the Mo_2C nanoribbon (a) and N-G (c) with different rates from 20 to 200 mV s^{-1} in 0.5 M H_2SO_4. The capacitive current at 0.2 V as a function of scan rate for Mo_2C nanoribbon (b) and N-G (d).

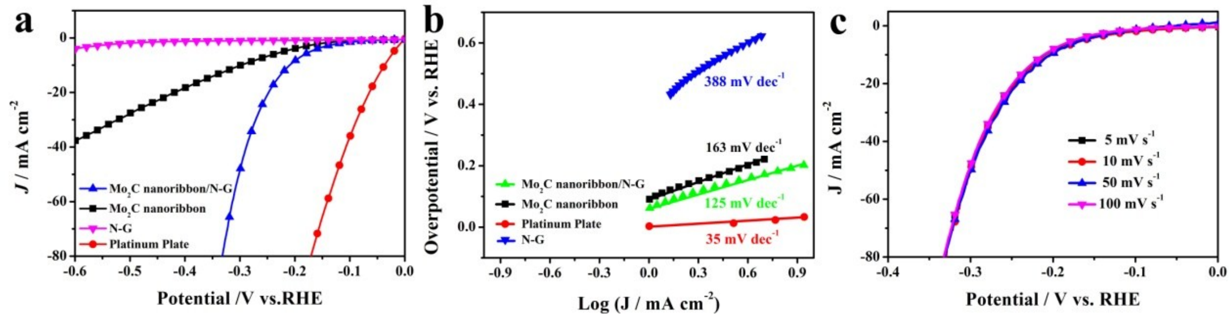

Figure S10 (a) HER polarization curves and (b) Tafel plots of Mo_2C nanoribbon/N-G, Mo_2C nanoribbon, N-G and Pt plate in the 1 M KOH, respectively. (c) HER polarization curves of Mo_2C nanoribbon/N-G at different scan rates.

Reference

1. C. Tang, L. Xie, X. Sun, A. M. Asiri and Y. He, *Nanotechnology*, 2016, **27**, 20LT02.
2. W. Gao, Y. Shi, L. Zuo, W. Fan and T. Liu, *Mater. Today Chem.*, 2016, **1**, 32-39.
3. X. Wang, *RSC Advances*, 2016, **6**, 31359-31362.
4. J. Wang, H. Zhu, J. Chen, B. Zhang, M. Zhang, L. Wang and M. Du, *Int. J. Hydrogen Energ.*, 2016, **41**, 18044-18049.
5. Y. Tan, P. Liu, L. Chen, W. Cong, Y. Ito, J. Han, X. Guo, Z. Tang, T. Fujita and A. Hirata, *Adv. Mater.*, 2014, **26**, 8023-8028.
6. Q. Dong, C. Sun, Z. Dai, X. Zang and X. Dong, *ChemCatChem*, 2016, **8**, 3484-3489.
7. L. Wang, Z. Sofer, J. Luxa, D. Sedmidubský, A. Ambrosi and M. Pumera, *Electrochem. Commun.*, 2016, **63**, 39-43.
8. Y. Zhao, K. Kamiya, K. Hashimoto and S. Nakanishi, *J. Am. Chem. Soc.* 2014, **137**, 110-113.
9. K. Zhang, Y. Zhao, D. Fu and Y. Chen, *J. Mater. Chem. A*, 2015, **3**, 5783-5788.
10. P. Xiao, Y. Yan, X. Ge, Z. Liu, J.-Y. Wang and X. Wang, *Appl. Catal. B Environ.*, 2014, **154**, 232-237.
11. W.-F. Chen, C.-H. Wang, K. Sasaki, N. Marinkovic, W. Xu, J. Muckerman, Y. Zhu and R. Adzic, *Energy Environ. Sci.*, 2013, **6**, 943-951.
12. H. Vrubel and X. Hu, *Angew. Chem. Int. Ed.*, 2012, **124**, 12875-12878.
13. L. Ma, L. R. L. Ting, V. Molinari, C. Giordano and B. S. Yeo, *J. Mater. Chem. A*, 2015, **3**, 8361-8368.
14. C. Ge, P. Jiang, W. Cui, Z. Pu, Z. Xing, A. M. Asiri, A. Y. Obaid, X. Sun and J. Tian, *Electrochim. Acta*, 2014, **134**, 182-186.
15. W. Cui, N. Cheng, Q. Liu, C. Ge, A. M. Asiri and X. Sun, *ACS Catal.*, 2014, **4**, 2658-2661.
16. N. S. Alhajri, D. H. Anjum and K. Takanabe, *J. Mater. Chem. A*, 2014, **2**, 10548-10556.